

Available online at [www.sciencedirect.com](http://www.sciencedirect.com)**ScienceDirect**

Energy Procedia 88 (2016) 341 – 348

Energy

**Procedia**

CUE2015-Applied Energy Symposium and Summit 2015: Low carbon cities and urban energy systems

## Case Study: Dynamic Performance of a MTDC Network in Zhoushan City

Z. Xu<sup>a,\*</sup>, C. Zhang<sup>b</sup>

<sup>a</sup>The University of Nottingham, China campus, 199 Taikang East Road, Ningbo, 315100, China

<sup>b</sup>State Grid Electric Power Research Institute (SGEPRI)

### Abstract

This paper presents dynamic responses of a multi-terminal high voltage DC (MTDC) network in Zhoushan islands, China. The conventional methods of controlling MTDC networks suffered from poor dynamic performance. In this paper, an optimal strategy is derived through three main steps: DC load flow, optimum power flow and N-1 security for MTDC networks. The strategy is fulfilled by incorporating the loss minimization in a MTDC network. The advantages of the strategy are verified by dynamic simulations using MATLAB/Simulink package.

© 2016 The Authors. Published by Elsevier Ltd. This is an open access article under the CC BY-NC-ND license (<http://creativecommons.org/licenses/by-nc-nd/4.0/>).

Peer-review under responsibility of the organizing committee of CUE 2015

*Keywords:* MTDC; dynamic responses; renewable energy; optimum power flow; N-1 security

### 1. Introduction

Future power systems will engage large number of power electronic interfaced renewable energy resources. Furthermore, the construction of a Pan-European high voltage DC transmission network, mainly utilized as bulk transmission system, will enable the inter-connection of previously asynchronous systems in a multi-terminal DC grid. Large offshore wind power plants will be incorporated into the MTDC grid.

In MTDC systems, multiple offshore wind power plants and onshore grids are interconnected through voltage source converters (VSCs) and long distance DC cables. To simplify the scheme, offshore wind power plants can be considered as power generation terminals to supply electricity for the entire onshore grids terminals. However, the wind energy is not sufficient perpetually like onshore power plants due to the intermittence of wind power, hence different dispatch demand is always provided among the onshore

\* Corresponding author. Tel.: +86-0574-88189135; fax: +86-0574-88180175.

E-mail address: [zhuang.xu@nottingham.edu.cn](mailto:zhuang.xu@nottingham.edu.cn).

grids consumption terminals. Despite of dispatch mechanisms in normal operation, some contingencies, such as the breakdown at a converter AC side, should be considered. Therefore, the control strategy should be capable of not only satisfying the different dispatch mechanisms during normal operation, but also performing acceptable operations when AC contingencies happen. To achieve the control of MTDC systems, two categories of control strategies which are voltage droop method and voltage margin method (VMM) are usually applied.

The principle of voltage droop method [1-3] for MTDC systems is straightforward and the fast communication is not required. However, it is difficult to apply this method for the fixed power sharing because the proportional controller is employed [4-6]. Due to the fact that the power distribution is adjusted through the assigned converter based on the instantaneous value of the DC voltage, the difficulty of the fixed power sharing is increased largely.

Generally, the voltage margin strategy [9-10] is achieved through the double-stage or single-stage controllers. Compared with the single-stage controller, the double-stage controller needs less communication between terminals and it is much more flexible [5]. As a result, the double-stage controller is a better alternative for multi-terminal networks. However, the VMM dynamic response time is longer than other strategies due to its controller structure, and the DC voltage is controlled by only one VSC at a time [6-8]. Additionally, because the DC voltage operating range is restricted, the system capability of controlling VSC terminals might be limited. In spite of these two drawbacks above, the fixed power sharing can be implemented by VMM.

Large multi-terminal DC networks should have the capability of steering the power flow inside DC networks by means of assigning each VSC terminal with a predefined direct voltage set-point. This could make any predefined load flow scenario possible where all converters are involved with balancing the power inside the transmission system. An optimal strategy based on distributed direct-voltage control is proposed to achieve this goal.

## 2. An Optimal Control Strategy

### 2.1. Optimal Power Flow (OPF)

The basic operation principle of the OPF is to acquire the optimal values of system parameters to improve system functions, such as system security, loss, overall generation cost or operational limitation.

To apply OPF for MTDC networks, the state variables ( $\mathbf{x}$ ) and the specified variables ( $\mathbf{z}$ ) are defined in the first place.

$$\mathbf{z} = [\mathbf{U} \ \mathbf{W}]^T \quad (1)$$

where:  $\mathbf{U}$  is control variables;  $\mathbf{W}$  is fixed variables.

In AC power systems, the state variables consist of the node phase angle and the nodal voltage on PQ-type buses, i.e.  $\mathbf{x} = [\delta_1, \dots, \delta_{N-1}, V_1, \dots, V_{N-1}]^T$ ; or only the node phase angle on PV-type buses, i.e.  $\mathbf{x} = [\delta_1, \dots, \delta_{N-1}]^T$ . In the DC networks, the state variables are represented as the nodal voltage on P-type buses, i.e.  $\mathbf{x} = [V_{dc1}, \dots, V_{dcN-1}]^T$ .

In terms of the specified variables ( $\mathbf{z}$ ), the control variables ( $\mathbf{U}$ ) are the DC pre-set voltage references, and the fixed variables ( $\mathbf{W}$ ) are the power generation and demand. Therefore, this OPF problem without inequality constraints can be considered as the minimization:

$$\begin{cases} \min f(\mathbf{x}, \mathbf{U}) \\ \mathbf{g}_p(\mathbf{x}, \mathbf{U}, \mathbf{W}) = 0 \end{cases} \quad (2)$$

where  $f(\mathbf{x}, \mathbf{U})$  is the optimized function;  $\mathbf{g}_p(\mathbf{x}, \mathbf{U}, \mathbf{W})$  is the load flow equation.

To solve the minimization problem above, the steepest descent gradient method is applied as the optimization method. The unconstrained Lagrangian function is constructed as:

$$L(\mathbf{x}, \mathbf{U}, \mathbf{W}) = f(\mathbf{x}, \mathbf{U}) + \boldsymbol{\lambda}^T \mathbf{g}_P(\mathbf{x}, \mathbf{U}, \mathbf{W}) \quad (3)$$

where  $L$  is the unconstrained Lagrangian function;  $\boldsymbol{\lambda}$  is the lagrangian multipliers vector.

The minimization situations of the Lagrangian function can be written as:

$$\begin{cases} \Delta L_{\mathbf{x}} = \frac{\partial L}{\partial \mathbf{x}} = \frac{\partial f}{\partial \mathbf{x}} + \left[ \frac{\partial \mathbf{g}_P}{\partial \mathbf{x}} \right]^T \cdot \boldsymbol{\lambda} = 0 \\ \Delta L_{\mathbf{U}} = \frac{\partial L}{\partial \mathbf{U}} = \frac{\partial f}{\partial \mathbf{U}} + \left[ \frac{\partial \mathbf{g}_P}{\partial \mathbf{U}} \right]^T \cdot \boldsymbol{\lambda} = 0 \\ \Delta L_{\boldsymbol{\lambda}} = \frac{\partial L}{\partial \boldsymbol{\lambda}} = \mathbf{g}_P(\mathbf{x}, \mathbf{U}, \mathbf{W}) = 0 \end{cases} \quad (4)$$

There are six main steps in the OPF with the steepest descent gradient method. Initially, the original value is assigned to the control vector ( $\mathbf{U}^0$ ), which means the slack node DC voltage is set as 1 pu. In the second step, the load flow equation is solved, i.e.  $\Delta L_{\boldsymbol{\lambda}} = \mathbf{g}_P(\mathbf{x}, \mathbf{U}, \mathbf{W}) = 0$ .  $\frac{\partial f}{\partial \mathbf{x}} + \left[ \frac{\partial \mathbf{g}_P}{\partial \mathbf{x}} \right]^T \cdot \boldsymbol{\lambda} = 0$ ,  $\boldsymbol{\lambda}$  can be derived as:

$$\boldsymbol{\lambda} = -[\mathbf{J}^T]^{-1} \frac{\partial f}{\partial \mathbf{x}} \quad (5)$$

Then plug state variables ( $\mathbf{x}$ ) and  $\mathbf{J} = \partial \mathbf{g}_P / \partial \mathbf{x}$  into (15), the lagrangian multipliers vector  $\boldsymbol{\lambda}$  can be found. In the next step, use the new value of  $\boldsymbol{\lambda}$  to find the  $\Delta L_{\mathbf{U}}$  through the second row in (14). Subsequently, check the absolute value  $\Delta L_{\mathbf{U}}$  with  $\varepsilon (10^{-12})$  which is the smallest value computer can recognize. If  $\Delta L_{\mathbf{U}}$  is greater than or equal to  $\varepsilon$ , the new control vector ( $\mathbf{U}^{m+1}$ ) is updated through:

$$\mathbf{U}^{m+1} = \mathbf{U}^m + \beta |\Delta L_{\mathbf{U}}| \quad (6)$$

After that, use the new control vector ( $\mathbf{U}^{m+1}$ ) to repeat the procedure above from the second step. If  $|\Delta L_{\mathbf{U}}|$  is smaller than  $\varepsilon$ , the optimization algorithm is completed. In conclusion, the state vector ( $\mathbf{x}$ ) which is the node DC voltage except the slack node is computed through the Newtown-Raphson method in the beginning, and then this state vector ( $\mathbf{x}$ ) and the initial control vector ( $\mathbf{U}^0$ ) are applied to compute the new control vector ( $\mathbf{U}^{m+1}$ ) through the steepest descent gradient method, and then repeat the procedure above until  $|\nabla L_{\mathbf{U}}|$  satisfies the limit condition.

## 2.2. N-1 Security

Although the power losses of the MTDC system are optimized through applying the steepest descent gradient method, some node DC voltages may surpass the device limit. To prevent the MTDC system from breaking down, N-1 security method is employed to guarantee that each VSC works under its rating conditions.

After OPF is achieved, it is required to check whether the obtained results satisfy the N-1 security or not. The system satisfies the N-1 security if, after arbitrary node voltages are examined, the node voltage in the VSC does not exceed its regulation constraints.

## 3. A Case Study: Zhoushan islands MTDC Transmission Project

### 3.1. Introduction

Zhoushan MTDC transmission project (China) employs the traditional VMM method to achieve the control functionalities. However, the dynamic responses are relatively slow because of its control nature and the fact that DC voltage is controlled by only one VSC at a time. In addition, the power efficiency and the response accuracy are relatively low. To solve the problems above, the novel control strategy is simulated and examined in the project.

Zhoushan transmission network layout is displayed in Figure 4.1.1. The map consists of five islands, namely Dinghai (DH), Daishan (DS), Qushan (QS), Yangshan (YS) and Sijiao (SJ). The three terminals (N01, N02, N03) are offshore wind farms (OWF) for power generation, three terminals (N09, N10, N11) are onshore power grids (OG) for power consumption, and two terminals (N12, N13) are slack terminals for controlling DC voltage. In addition, twelve DC transmission cables are shown in Table 4.1.1.

The resistance of unit length is  $0.23\Omega/\text{km}$ , the DC network voltage base is  $\pm 200\text{kV}$  - which is also the rated DC voltage for HVDC terminals, and the system base power is set as 100MVA.

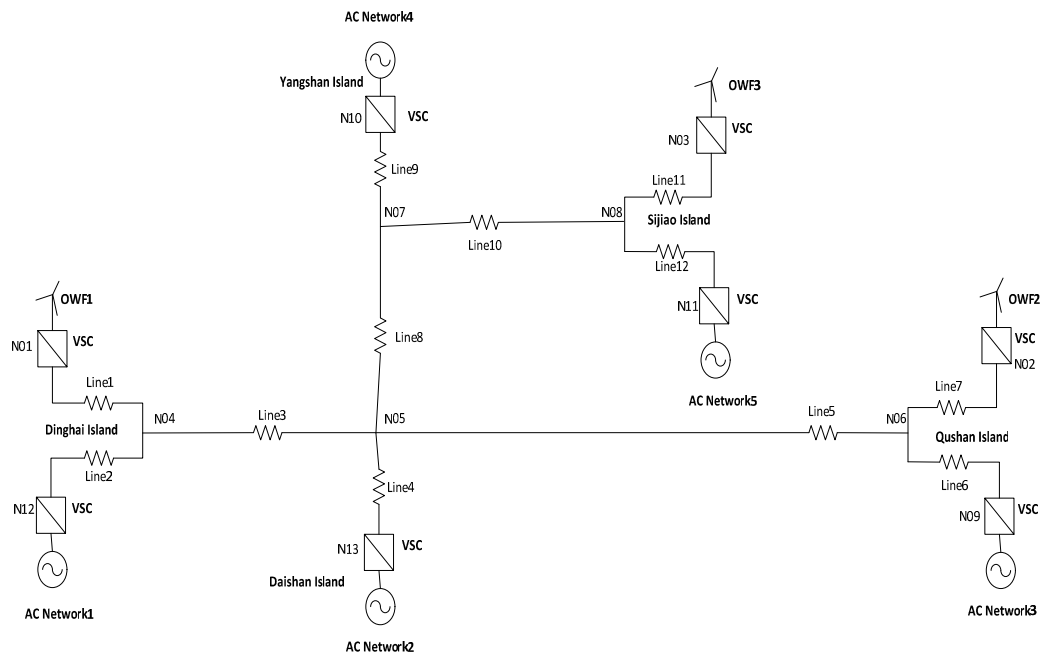


Fig. 1. Zhoushan 8-terminal VSC-MTDC Network Layout

### 3.2 Dynamic performance

The S-function in MATLAB was utilized to simulate the dynamic power conditions. Three step inputs were used to simulate the dynamic wind power, where DH OWF generated 3 pu power in 0.1s, QS OWF generated 2 pu power in 0.2s and SJ OWF generated 1 pu power in 0.3s. To simulate the AC contingency, QS onshore VSC was faulted between 0.7s and 0.8s, and YS onshore VSC was faulted between 0.765s and 0.9s, which means both QS and YS onshore VSCs were faulted between 0.765s and 0.8s. In addition, the power consumption was 1 pu in QS, YS, SJ OGs respectively during the normal operation, and DH, DS OGs were selected as slack nodes. In addition, all OWFs are regarded to be generating 75% of their nominal power, while all onshore grids are regulating their power to match the power generation from OWFs. In the input side, three power generation terminals and two faulted consumption terminals are

depicted, while in the output side, all terminals are displayed. Moreover, the middle HVDC block represents the optimization and N-1 security algorithm for the whole system. Figure 2 illustrates the integration and interaction between offshore wind farms and other system components through the modular representation.

Figure 3 displays the active power changes of OWFs and OGs during different periods in one second, where the horizontal axis represents the time and the vertical axis represents the active power in pu. Due to the intermittence of the wind power and faulted onshore grid VSCs, the power variation diagrams of the slack nodes are shown in the Figure. When the power generation was insufficient, the active power was positive in the slack node, which meant the slack node acted as a power supplier in the system. However, when the power generation was sufficient, the active power was negative in the slack node, which meant the slack node acted as a power consumer in the system. The aim of the active power variation in slack nodes was to satisfy the power requirement with a relatively low system transmission loss.

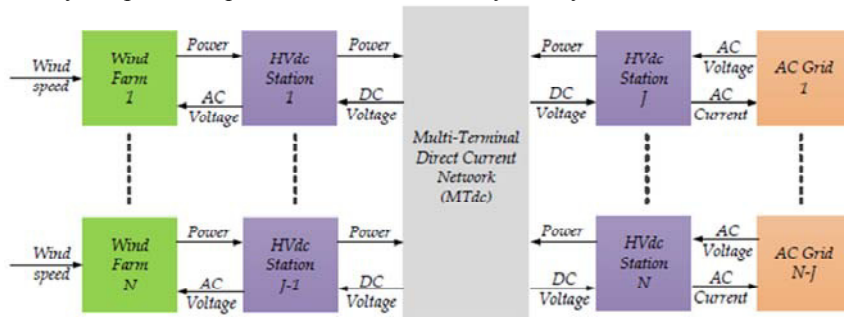


Fig. 2. Modular Representation of the MTDC System

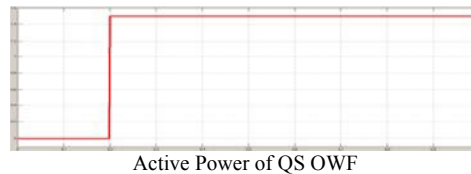
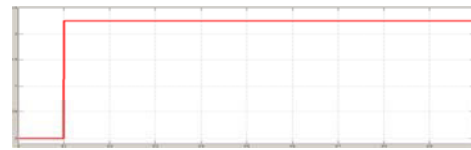




Fig. 3. Dynamic active powers of OWFs and OGs



Fig. 4. Power Losses of the whole system

Figure 4 and Table 1 show the MTDC system transmission power loss during different periods in one second irrespective of the loss in VSCs, where the horizontal axis represents the time and the vertical axis represents the total transmission power loss. The maximum number of the system transmission power loss was 4.24% which was between 0 and 0.1s, while the minimum number was 0.6% between 0.8s and 0.9s. In contrast with the DC voltage curve, it could be demonstrated that a larger DC system voltage profile would contribute to a lower system transmission power loss. Consequently, optimization and N-1

security algorithm was to control the DC voltage as high as possible to minimize the system loss but guarantee VSCs under the operation limit condition (1.10 pu).

Table 1 Power Loss of the whole system

Time [s]	System Transmission Power Loss [%]
0-0.1	4.24
0.1-0.2	4.04
0.2-0.3	4.02
0.3-0.7	1.24
0.7-0.769	2.23
0.769-0.8	1.35
0.8-0.9	0.6
0.9-1.0	1.24

## Conclusions

An optimal control strategy has been developed such that several nodes are responsible for controlling the DC network voltage instead of a single converter node. Load flow results and dynamic simulations have verified the correctness of the control strategy for large MTDC systems.

Authors keep full copyright over papers published in Energy Procedia

## Acknowledgements

The authors would like to thank Ningbo Science and Technology Bureau China for the financial support of this very interesting project (2013D10012).

## References

- [1] Coil Innovation Power Inductors. CI awarded contract for “Caprivi” HVDC Smoothing Reactors. Last Accessed: 07 September, 2013. [Online]. Available: <http://www.coilinnovation.com/company/news-archive/?L=1>
- [2] B. K. Johnson, R. H. Lasseter, F. L. Alvarado, and R. Adapa, “Expandable multiterminal DC systems based on voltage droop,” *IEEE Trans. Power Del.*, vol. 8, no. 4, pp. 1926–1932, Oct. 1993.
- [3] T. Haileselassie and K. Uhlen, “Impact of DC Line Voltage Drops on Power Flow of MTDC Using Droop Control,” *IEEE Transactions on Power Systems*, vol. 27, no. 3, pp. 1441–1449, 2012.
- [4] R. Teixeira Pinto, P. Bauer, S. Rodrigues, E. Wiggelinkhuizen, J. Pierik, and B. Ferreira, “A Novel Distributed Direct-Voltage Control Strategy for Grid Integration of Offshore Wind Energy Systems Through MTdc Network,” *IEEE Transactions on Industrial Electronics*, vol. 60, no. 6, pp. 2429–2441, June 2013.
- [5] EWEA. The European Wind Energy Association Report, “Eastern winds. Emerging European Wind Power Markets” in February 2013. Available online at: <http://www.ewea.org/>
- [6] D. Jovicic, “Interconnecting offshore wind farms using multi-terminal VSC-based HVDC,” *IEEE PES General Meeting*, 2006
- [7] Meah, K.; Ula, S., "Comparative Evaluation of HVDC and HVAC Transmission Systems," *Power Engineering Society General Meeting*, 2007. *IEEE*, vol., no., pp.1, 5, 24-28 June 2007.

[8] N. Flourentzou, V. G. Agelidis, and G. D. Demetriades, “VSC-Based HVDC Power Transmission Systems: An Overview,” *IEEE Trans. Power Electronics*, vol. 24, no. 3, March 2009, pp. 592-602.

[9] Y. Tokiwa, F. Ichikawa, K. Suzuki, H. Inokuchi, S. Hirose, and K. Kimura, “Novel control strategies for hvdc system with self-contained converter,” *Electrical Engineering in Japan*, vol. 113, no. 5, pp. 1–13, 1993. [Online]. Available: <http://dx.doi.org/10.1002/ej.4391130501>

[10] L. Livermore, J. Liang, and J. Ekanayake, “MTDC VSC Technology and its applications for wind power,” in *Proc. 45th Int. UPEC*, Aug. 31–Sep. 3, 2010, pp. 1–6.



### **Biography**

Dr Zhuang Xu works with the University of Nottingham Ningbo China. Zhuang Xu received his Ph.D. degree in electrical engineering from the University of New South Wales, Sydney, Australia. His research has been focused on power electronics and high performance electrical drives.